Validation of a passive beam Monte Carlo model for measuring prompt gamma rays during proton radiotherapy

[1]**Jeyasingam Jeyasugiththan,** [1]**Stephen Peterson,** [2]**Jaime Nieto Camero and** [2]**Julyan Symons**

[1]Department of Physics, University of Cape Town, Rondebosch, 7701, South Africa
[2]Medical Radiation Division, iThemba L.A.B.S., Faure, 7131, South Africa

E-mail: jeyasugiththan@yahoo.com

Abstract. In proton beam radiotherapy, secondary gamma rays are produced by proton-nuclei inelastic collisions within the treatment volume. A Monte-Carlo model of the iThemba proton treatment nozzle was developed using the Geant4 toolkit to detect these secondary or prompt gamma rays, which could be used for on-line treatment verification. The passive beam proton treatment facility at iThemba Labs in Cape Town, South Africa was studied in detail and all the nozzle components that interact with the proton beam were built and positioned in the model at the locations specified by the manufacturer. NaI detectors with different dimensions were modeled and standard gamma emitting sources in the energy range from 0.661 to 4.438 MeV were used to determine the detector response. The simulated treatment nozzle was validated against depth dose and lateral profiles in a water phantom for different therapeutic proton ranges. The position of the graphite double wedge energy degrader was calibrated within the model. Range uncertainties due to secondary production energy threshold were measured in detail. Our Geant4 treatment nozzle model is in good agreement with measurements and has the ability to produce depth dose profiles and lateral profiles for different proton ranges. Lastly simulations to detect prompt-gammas produced in a water phantom were performed and will be validated with future experimental measurements

1. Introduction

Protons have a finite range in material compared to the exponential attenuation of photons. This difference has been used to develop proton radiation therapy, where proton therapy has exhibited significant dose control and tissue sparing compared to traditional photon therapy. These properties of protons also require a more precise delivery of the radiation, which is hindered by the absence of primary particles exiting the patient for verification purposes. One option is to use secondary radiation for dose verification purposes, like prompt gammas produced by proton-nuclei inelastic collisions [1]. This work is developing a Monte Carlo model of the proton beam line at iThemba Labs in order to validate on-going prompt-gamma measurements.

2. Geant4 passive beam line model

In the passive beam proton therapy treatment technique, an accelerated mono-energetic proton beam is directed into a treatment nozzle where a single or double beam scattering method is

used to broaden the proton beam uniformly in the lateral direction by placing high-Z scattering plates into the beam path. The beam can also be spread out along the beam direction to form a spread out Bragg peak (SOBP) with the use of a range modulator wheel. In addition, there is a set of collimators in place to spare the patent and electronics from excess scattered radiation by the beam-line elements. Our passive beam line model is built using the Geant4 [2] Monte Carlo (v9.6) code. Geant4 is an object oriented and open source C++ toolkit used to simulate particles travelling through a medium, and has been used to compute proton treatment nozzle by many researchers [3], [4].

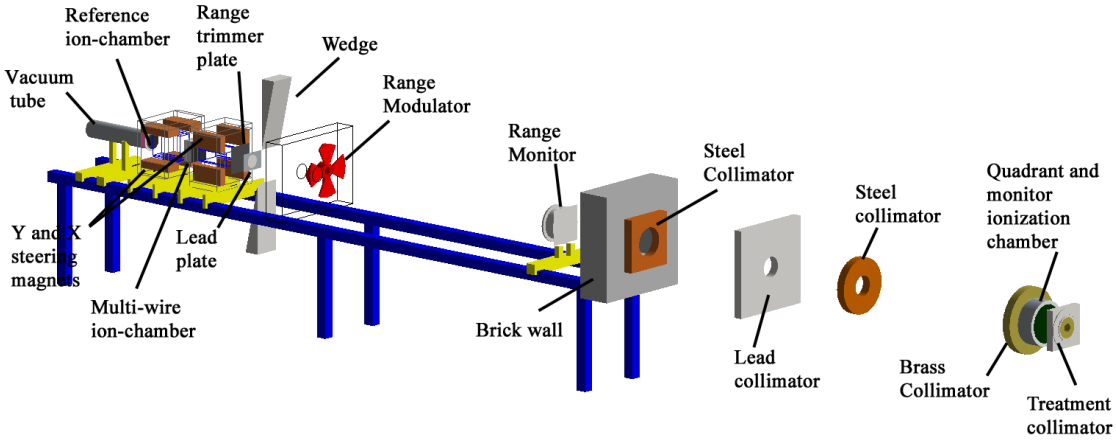

Figure 1: Geant4 Monte Carlo model of the proton passive beam line at iThemba Labs.

The entire Monte Carlo beam model is shown in the Figure 1, including all elements that directly interact with the beam. The vacuum chamber is the first element in the treatment nozzle. The reference ionization chamber which was placed next to the vacuum tube acts as the first scatterer. The lead plate or graphite double wedge degrader is the second scatterer (see Figure 2(a)). The double wedges are mounted back to back on a drive mechanism that allows them to slide up and down parallel to each other in opposite directions. Therefore the thickness of the double wedge energy degrader at the beam axis varies in order to produce different proton ranges at the isocenter. The maximum range (R_{50}), measured at the 50% distal edge of the Bragg peak, that can be produced using the wedges is 220 mm. The R_{50} range for the open position of the wedges (shooting through the lead plate) is 240 mm. The range monitor which is a vacuum chamber that consists of a multi-layer Faraday cup (MLFC), a brass occluding rod and a steel scattering plate is responsible for producing the lateral dose profile. Figure 2(b) illustrates the distribution of energy deposited by the proton beam within the range monitor. Protons traveling through the occluding rod are completely stopped in order to produce a uniform lateral dose distribution.

Geant4 provides a complete physics process model for electromagnetic and hadronic interactions that can be modified at the user's convenience. In this study, we adapted the physics model using G4VModularPhysicsList class that allows the definition of all the pre-packaged Reference physics lists. We have chosen the recommended QGSP_BIC_EMY reference physics list, validated for proton and ion beam radiotherapy [5]. The accuracy of particle tracking depends on two factors: RangeCut(energy threshold) and StepMax(maximum step size). In our beam line model, the particle step size of 0.01 mm was set inside the water phantom and the remaining regions. The step limit of 0.01 mm is good enough to ensure adequate energy deposit within each detector slice and smaller than thickness of the slice. The range cut was set to

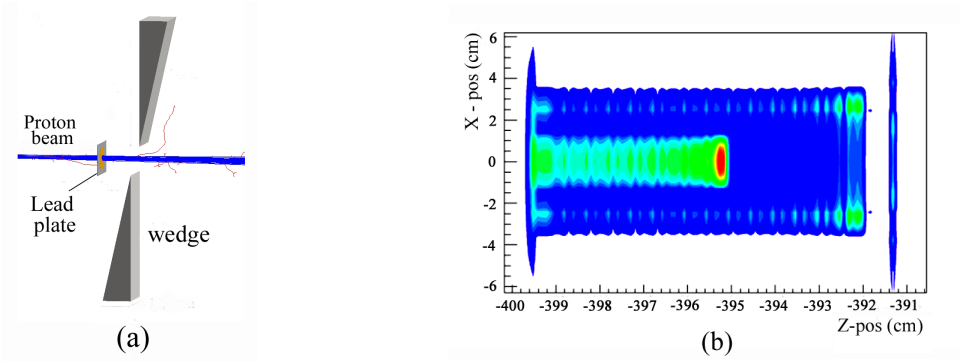

Figure 2: *(a) The double wedge energy degrader and lead plate system (b) Distribution of energy deposited within the range monitor.*

0.01 mm, which is translated into an equivalent minimum energy threshold for each type of the simulated particles. The primary particles were generated using Geant4 General Particle Source package(GPS).

3. Validation of passive beam Monte Carlo model

In order to validate the Geant4 model of the proton beam line, it must be able to replicate the dose profiles used for the treatment of patients, specifically the depth dose and lateral dose profiles. The iThemba proton beam line is calibrated before every treatment by measuring the range of the beam, measured at the 50% distal falloff position in water (R_{50}). Range trimmer plates are added or removed from the beam to adjust for variations in the beam until the 50% distal position is at 24 cm. For the Monte Carlo model, instead of working backwards from a 24 cm range, we must start with a detailed description of the incoming beam of protons. The expected proton energy exiting the vacuum window into the treatment room is 199.78 MeV, but this value was adjusted to 201.36 MeV in order for our simulations to line up with the measured values.

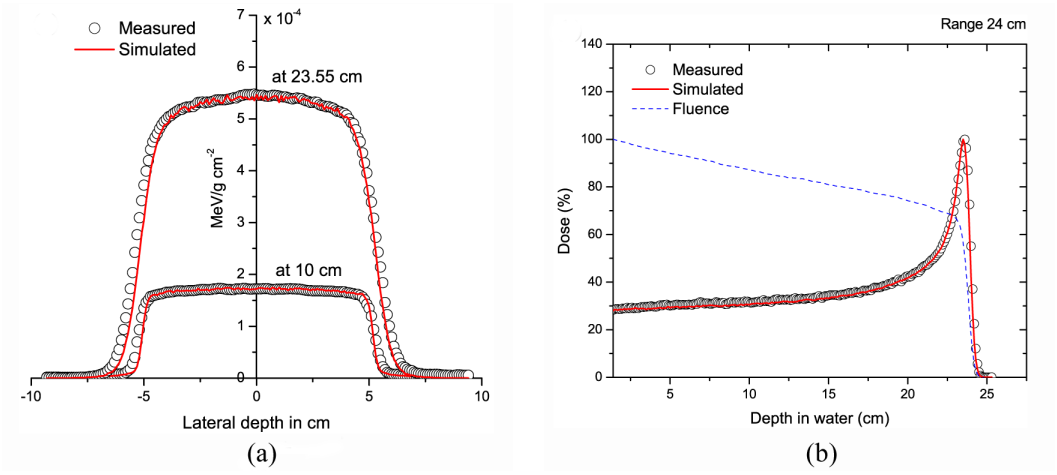

Figure 3: *Comparison of measured and simulated data using adjusted beam energy (a) lateral dose profile at the depth of 10 cm and 23.55 cm and (b) Bragg peak.*

Measured depth dose and lateral dose data were used to validate the beam line model. The simulation measurements were performed in a voxelized region created within the water phantom using the ROGeomtry classes. The volume of each cubic voxel is 0.01 cm^3, which is equal to the effective volume of the ionization chamber typically used at iThemba Labs for the beam calibration. The energy deposited by both primary protons and secondary radiation in each voxel was collected at the end of each run. Figure 3(b) is comparing the simulated Bragg curve with adjusted energy (201.36 MeV) normalized to the 100% dose level while Figure 3(a) is comparing the lateral dose profile at 10 cm and 23.55 cm (at the Bragg peak). The agreement between the simulated and measured data is within 0.3%.

3.1. Validation of double wedge degrader

For ranges less than 24 cm, the double wedge degrader is used to reduce the energy of the beam. The vertical wedge position (WP) of the double wedge degrader was calibrated against different proton ranges within the model. The following relationship was obtained by linear fitting the data as shown in the Figure 4(a).

$$WP(mm) = \frac{Range - a}{b} \tag{1}$$

where a and b are constants ($a = 9.39337 \pm 0.00238$ cm and $b = 0.74359 \pm 0.00025$). Figure 4(b) shows the comparison of simulations against experimental results for different proton ranges in water. The agreement between the simulated and measured data for different wedge positions is within 0.5% for proton ranges between 22 and 5 cm.

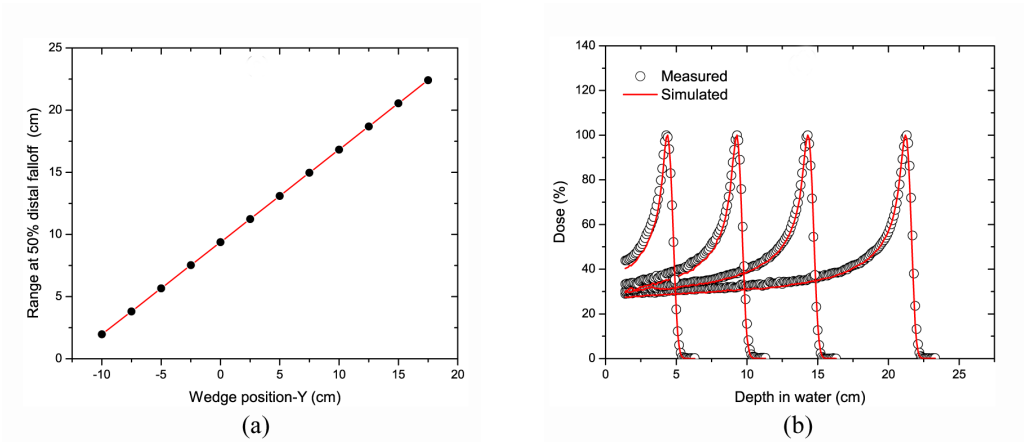

Figure 4: (a) Proton range as a function of wedge position and (b) comparison of relative dose profile with measurement for 22.73, 14.75, 9.7 and 4.72 cm ranges.

3.2. Effect of the mean excitation energy

In Geant4, the continuous energy loss per step in a track is based on restricted stopping power calculated using the Bethe-Bloch formula. In the Bethe-Bloch equation, the energy deposition per unit length is strongly dependent on both density and mean excitation energy[1] (MEE) of the target material. Moreover, the mean excitation energy can be approximated by $MEE = (10$

[1] also called mean ionization potential

eV)Z, where Z is the atomic number of the material. The ICRU-recommended MEE value for water is 75 ± 3 eV [6]. The uncertainty on the MEE value can not be ignored because other authors have reported slightly different values: 80 ± 2 eV [7] measured relative to Al using Bragg curves, 81.8 eV [8] which was used to produced stopping power tables, 77 eV [9] obtained by matching the measured Bragg peaks of carbon-ion and 78.4 ± 1.0 eV [10] which was determined from the proton beam ranges in water. Furthermore, a 0.8 - 1.2% [10] variation in the stopping powers was reported to have the same impact on the absorbed dose for MEE values between 75 and 80 eV in the energy range of 10 - 250 MeV. Andreo(2009) studied the variation of the Bragg peak with different mean excitation energy of water and the composition of organs and tissue for pencil beam of protons and carbon [11].

Table 1 : A summary of calculated $R_{50\%}$ values corresponding to different MEE of water for proton of 240 mm range. Measured value is 240.1 mm ($^{m}R_{50\%}$).

IEnergy (eV)	^{IE}R$_{50\%}$ (mm)	$^{m}\Delta R_{50\%}$ (mm)	$^{s}\Delta R_{50\%}$ (mm)	%
67	232.86	7.2	-3.2	-1.3
70	234.05	6.0	-2.0	-0.8
72	234.86	5.2	-1.2	-0.5
73	235.24	4.9	-0.8	-0.3
75	236.04	4.1	0	0
77	236.82	3.3	0.8	0.3
78	237.19	2.9	1.2	0.5
80	237.85	2.2	2.0	0.8
81	238.27	1.8	2.2	0.9
83	238.99	1.1	2.95	1.2
84	239.33	0.8	3.3	1.4
86	240.03	0.1	4.0	1.7
90	241.40	-0.3	5.4	2.3

$^{m}\Delta R_{50\%} = {}^{m}R_{50\%} - {}^{IE}R_{50\%}$
$^{s}\Delta R_{50\%} = {}^{IE}R_{50\%} - {}^{75}R_{50\%}$

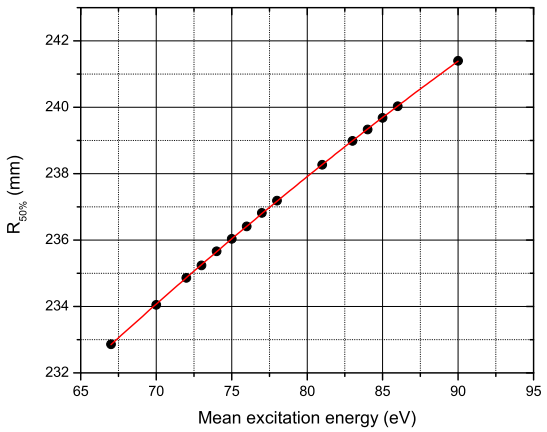

Figure 5: *Range as a function of mean excitation energy of the water.*

Table 1 summarizes the simulated proton ranges for different MEE values. The calculated ranges were then compared to the measured proton range of 240.1 mm. Protons starting with an initial energy of 199.78 MeV lose energy along the beam line in both the scatterers as well as the energy degrader. The mean proton energy exiting the final patient collimator and reaching the target was measured to be 188.6 MeV or producing an equivalent range of 23.5 cm (0.4% from the expected value of 24 cm). As shown in figure 5, the appropriate MEE value to produce a 24 cm range (with a 199.78 MeV starting proton energy) is 85.9 eV. This MEE value fell outside of the expected range of values discussed above, so the ICRU-recommended value of 75 eV was used and a readjustment to the proton beam of 1.58 MeV was used to compensate for the lower MEE value. The corrected beam energy was 201.36 MeV.

4. Validation of NaI detector

The detector response function is essential to generate the actual detector spectral responses of the prompt gamma in the Geant4 Monte Carlo simulation. The ideal mono-energetic gamma ray spectrum is a sharp line at the energy of the incident gamma (E) as shown in Figure 6(a), but due to statistical fluctuations in the number of electron-ion pairs produced by the photo-electron and Doppler broadening during the proton-nuclei collisions, the actual gamma ray spectrum has a Gaussian shape as shown in Figure 6(a).

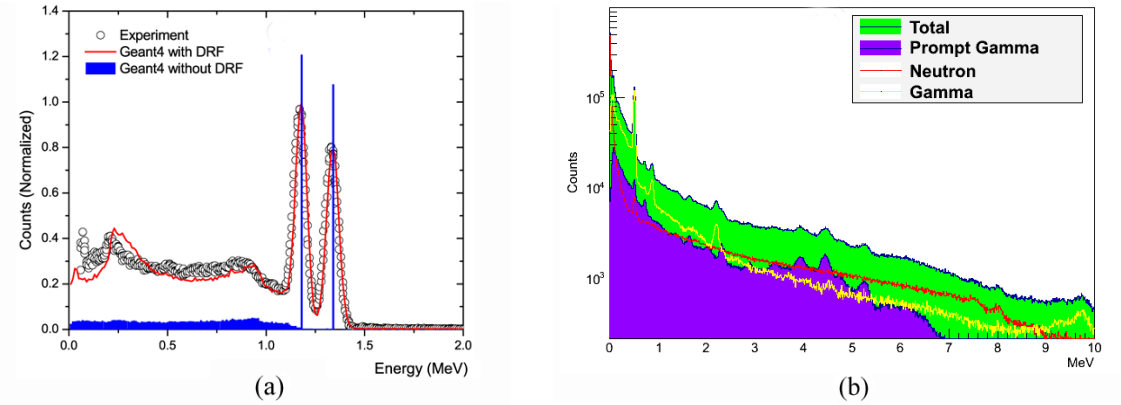

Figure 6: (a) Comparison of measured ^{60}Co spectra and simulated ^{60}Co spectra with and without the detector response function of a 3 x 3 inch NaI detector. (b) Simulated prompt gamma spectrum measured in water by a 3 x 3 inch NaI detector.

Each detector has a unique response to these factors, thus producing slightly different energy resolution values. The parameter FWHM (full width of the photo peak at half its maximum) measures the detector energy resolution. A higher resolution detector has a smaller value of FWHM. If the shape of the photo peak is a standard Gaussian shape, the FWHM is given by

$$FWHM = \sigma\sqrt{8ln2} \tag{2}$$

The standard deviation σ of the Gaussian shape depends on the energy of the detected gamma ray. This relationship $\sigma = xE^y$ was reported as a good choice to determine the detector response because of its simplicity [12], where E is the incident particle energy. The parameters x and y were determined by measured the energy resolution of the specific detector to be used for the prompt gamma measurements. Standard gamma emitting sources with an energy range from 0.661 to 4.438 MeV were used for the detector resolution calibration. The detector response was then validated against the measured energy spectra of different radioactive sources. The comparison between simulation (with and without detector response) and experimental energy spectra of ^{60}Co point source for 3 x 3 inch NaI detector is shown in the Figure 6(a). The Geant4 generated detector response agree with experiment well in the photo peak and Compton edge energy regions. The differences in the lower energy region could be due to the contribution of scattered gamma rays from surrounding objects that were not modeled in the simulation.

5. Validation for prompt gamma measurements

Although the prompt gamma measurements are on-going, these validation simulations have been used as a preliminary expectation of results and to assist in the set-up of the experimental measurements. Simulations were carried out to detect prompt-gammas produced in the water phantom by a 24-cm proton beam. The simulated prompt-gamma spectra (shown in Figure 6(b)) shows the various peaks for ^{12}C, ^{14}N and ^{16}O at 0.73, 1.02, 1.98, 2.31, 2.74 and 4.44 MeV. In addition, a strong 0.511 MeV gamma peak produced by positron annihilation was observed. The single and double escape peaks of the 4.44 MeV gamma-ray from ^{12}C are clearly seen within the energy range between 3.0 and 5.0 MeV. Once the experimental data measuring the prompt gammas have been completed, these simulations will be updated to reflect the actual detector set-up as well as any other changes required to ensure the Geant4 model mimics the measured results.

6. Conclusion

Our Geant4 treatment nozzle model is in good agreement with treatment-relevant measurements and has the ability to produce depth dose and lateral profiles at different proton ranges. Moreover, the model has produced promising prompt gamma results that are currently being pursued with measurements at iThemba Labs. The physics model for prompt gamma emission will be validated against the experimental results and energy spectra will then be compared with measured data.

Acknowledgments

The authors would also like to thank the Center for High Performance Computing (CHPC), CSIR Campus, 15 Lower Hope St., Rosebank, Cape Town, in South Africa for providing them access to their clusters and resources.

References

[1] Polf J C, Peterson S, Ciangaru G, Gillin M and Beddar S 2009a *Phys. Med. Biol.* **54** 731

[2] Agostinelli S, Allison J, Amako K and Apostolakis J 2003 *Nucl. Instrum. Methods Phys. Res.* **A 506** 250–303

[3] Parodi K, Paganetti H, Shih H A, Michaud S, Loeffler J S, Delaney T F, Liebsch N J, Munzenrider J E, Fischman A J, Knopf A and Bortfeld T 2007 *Int J Radiat Oncol Biol Phys.* **68** 920–934

[4] Peterson S W, Polf J, Bues M, Ciangaru G, Archambault L, Beddar S and Smith A 2009 *Phys. Med. Biol* **54** 3217–3229

[5] Cirrone G A P, Cuttone G, Mazzaglia S E, Romano F, Sardina D, Agodi C, Attili A, Blancato A A, Napoli M D, Rosa F D, Kaitaniemi P, Marchett F, Petrovic I, Ristic-Fira A, Shin J, Tarnavsky N, Tropea S and Zacharatou C 2011 *Progress in nuclear science and technology* **2** 207–212

[6] ICRU 1993 Stopping powers and ranges for protons and alpha particles International Commission on Radiation Units and Measurements,Bethesda, MD ICRU Report 49

[7] Bichsel H and Hiraoka T 1992 *Nucl. Instrum. Methods Phys. Res. B* **66** 345–51

[8] Janni J F 1982 *At. Data Nucl. Data Tables* **27** 147–529

[9] Krmer M, Jkel O, Haberer T, Kraft G, Schardt D and Weber U 2000 *Phys. Med. Biol* **45** 3299–3317

[10] Kumazakia Y, Akagib T, Yanoua T, Suga D, Hishikawa Y and Teshimac T 2007 *Radiat. Meas.* **42** 1683–91

[11] Andreo P 2009 *Phys. Med. Biol* **54** N205–N215

[12] Wang J, Wang Z, Peeples J, Yu H and Gardner R P 2012 *Applied Radiation and Isotopes* **70** 1166–74